Physica B 407 (2012) 4027–4031

Contents lists available at SciVerse ScienceDirect

Physica B

journal homepage: www.elsevier.com/locate/physb

Enhancement of room temperature sub-bandgap light emission from silicon photonic crystal nanocavity by Purcell effect

A. Shakoor [a,*], R. Lo Savio [b], S.L. Portalupi [b], D. Gerace [b], L.C. Andreani [b], M. Galli [b], T.F. Krauss [a], L. O'Faolain [a]

[a] SUPA, School of Physics and Astronomy, University of St. Andrews, North Haugh, St. Andrews, Fife KY16 9SS, Scotland, United Kingdom
[b] Dipartimento di Fisica "A. Volta," Università di Pavia, 27100 Pavia, Italy

ARTICLE INFO

Available online 26 December 2011

Keywords:
Silicon light emission
Photonic crystal
Defect luminescence
Silicon photonics
Nanocavity
Purcell effect

ABSTRACT

We report the enhancement of sub-bandgap photoluminescence from silicon via the Purcell effect. We couple the defect emission from silicon, which is believed to be due to hydrogen incorporation into the lattice, to a photonic crystal (PhC) nanocavity. We observe an up to 300-fold enhancement of the emission at room temperature at 1550 nm, as compared to an unpatterned sample, which is then comparable to the silicon band-edge emission. We discuss the possibility of enhancing this emission even further by introducing additional defects by ion implantation, or by treating the silicon PhC nanocavity with hydrogen plasma.

1. Introduction

With the ever-increasing demand for data, the use of electronics is being pushed to its limits. The quest for higher processing speed and bandwidth has raised the interest of using photons instead of electrons for data transmission. To achieve an efficient photonic based data processing system, it is desirable to have a high on-chip integration density of components. As in electronics, it would be ideal to have a single material platform in order to achieve a high integration density of components and the integration of all essential functionalities on the same chip. The most attractive candidate to act as a material platform for such photonic chips is silicon, yet silicon is still missing a key component, namely a native light source.

The lack of such a silicon light source is due to the indirect bandgap of silicon, which makes it a poor emitter of light and there is a real need for enhancing the light emission from silicon to enable it to be used as a material for building light sources. Ideally, for large scale on-chip integration, the light source should be efficient, small, should operate at room temperature and allow electrical injection.

There has been a significant effort over the years to increase the light emission efficiency of silicon and a number of silicon light emitting devices have been reported [1–3]; none of these combines all of the desired properties, however. Examples of techniques used to increase light emission from silicon include the incorporation of rare earth ions such as erbium [4,5] but erbium requires low temperature operation given that the emission from rare earth ions at room temperature is completely quenched. Other techniques limited by the operating temperature are the luminescence from defects in silicon [1,6–8]. One of the few techniques that have demonstrated sizeable room-temperature emission is the creation of dislocation loops [2], but the device reported in this work, operated close to the silicon band-edge in addition to producing broadband emission, making it unsuitable for silicon-based optical interconnects. Similarly, the lasing action from silicon via the Raman effect [3] is a remarkable achievement but it is limited by the relatively large device size (centimetre scale) making large scale integration of such devices rather challenging, in addition to requiring an optical pump. In contrast, nano-size silicon light emitters based on photonic crystal nanocavities and operating at room temperature have already been demonstrated [9–11], but they typically operate at emission wavelengths that are lower than the band-edge. All of these techniques have major shortcomings, and there is a clear need for making a light source that is native to silicon and efficient, small sized, operates at room temperature and could be pumped electrically.

Here we report on a type of silicon nano-emitter that exhibits emission at 1.5 μm and that is comparable in brightness to the silicon band-edge emission. The features of this nano-emitter include small size, narrow line width (<1 nm), room temperature operation and the possibility of electrical excitation. This device exploits the Purcell effect, which enhances the emission from optically active defects in silicon via a photonic crystal nanocavity.

* Corresponding author. Tel.: +44 1334463091; fax: +44 1334463104.
E-mail address: as829@st-andrews.ac.uk (A. Shakoor).

0921-4526/$ - see front matter © 2011 Elsevier B.V. All rights reserved.
doi:10.1016/j.physb.2011.12.115

2. Purcell effect

According to Purcell [12], the spontaneous emission of an emitter is modified by the environment around it due to the change of its local density of states. Coupling the emitter with a cavity enhances its spontaneous emission, provided that there is a spectral and spatial overlap of the emission with the cavity mode. The factor by which the spontaneous emission is enhanced is referred to as the Purcell factor and is expressed by the following equation for a single emitter with dipole moment '*d*' [13,14]:

$$F_p = \frac{3Q_{eff}(\lambda_c/n)^3}{4\pi^2 V}\left|\frac{\vec{d}\,.\,\vec{f}\,(\vec{r}_e)}{\vec{d}}\right|^2 \frac{\Delta\omega_c^2}{4(\omega_e-\omega_c)^2+\Delta\omega_c^2} \quad (1)$$

where $1/Q_{eff}=1/Q_c+1/Q_e$ is the effective quality factor, taking into account the cavity *Q*-factor as well as the finite linewidth of the emitters [14], and *V* is the cavity mode-volume. The subscripts *c* and *e* stand for cavity and emitter, respectively. The second and third terms in this equation refer to the degree of spatial and spectral overlaps between the emitter and cavity mode, respectively. Usually, these factors are less than unity but by assuming perfect spatial and spectral overlaps, the Purcell factor reduces to the well known expression [12]:

$$F_p = \frac{3Q_{eff}(\lambda_c/n)^3}{4\pi^2 V} \quad (2)$$

This equation highlights that, in order to have a high Purcell factor and a corresponding enhancement of emission from the emitter, we require a coupled cavity–emitter system with a very high *Q*-factor and a small mode volume.

3. Experiments

To achieve a high Q_c/V value, we use a PhC with three missing holes, typically referred to as an L3 PhC nanocavity. The holes adjacent to the cavity are reduced in size and displaced laterally to increase the *Q*-factor of the cavity via the gentle confinement mechanism [15,16]. In addition, some of the holes around the cavity have been increased in size in order to form a second order grating, such that some of the *k*-vectors outside the vertical light emission cone are folded back, thus increasing the vertical far field emission efficiency [17,18]. These L3 PhC cavities can have *Q* values of the order of 10^5 and a very small mode volume, of the order of $V=(\lambda/n)^3$, thus achieving the desired high Q/V value.

The PhC cavity samples were fabricated on silicon on insulator (SOI), which was manufactured by the Smart Cut™ process and purchased from SOITEC. The top silicon layer was 220 nm with a 2 μm buried oxide layer. The fabrication was carried out by e-beam lithography, followed by reactive ion etching. The underlying silica layer was then removed with hydrofluoric acid to create a free standing PhC cavity membrane. The scanning electron microscope (SEM) image of fabricated PhC cavity samples is shown in inset of Fig. 2b.

Photoluminescence (PL) measurements were carried out at room temperature with a continuous wave Nd-YAG laser operating at 532 nm. The laser was focussed very tightly (1 μm) on the cavity with the help of an objective with a numerical aperture of $NA=0.8$. This excitation creates carriers that recombine radiatively at the defects that form midgap states (Fig. 1b). These defects are point-like, hence very narrow in real space and very broad in momentum space and can provide difference in momentum between the carriers, allowing the emission of photons [6,19–21]. This interpretation of defect-mediated radiative recombination of carriers to emit photons is shown in Fig. 1.

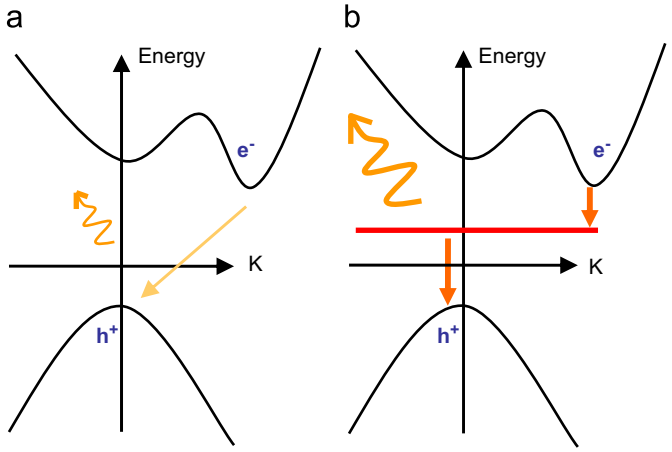

Fig. 1. Indirect bandgap of silicon: (a) due to the momentum mismatch, the probability of emission of photon is small and (b) the presence of a midgap point defect facilitates radiative recombination by momentum conservation due to its broadness in momentum space (red horizontal line). (For interpretation of the references to colour in this figure legend, the reader is referred to the web version of this article.)

4. Results and discussion

The defects discussed in previous section are believed to be created by the implantation of hydrogen during the manufacturing process of SOI via the Smart Cut™ method. The hydrogen implantation is carried out to create blistering, flaking and exfoliation of silicon. The creation of a blistered silicon layer helps to break off the implanted layer from the handle wafer after it is flip-bonded onto it. Although annealing of SOI at 1100 °C is part of the Smart Cut™ process, which anneals out most of these defects, yet some of them do remain in the top silicon layer. The presence of these defects significantly increases the PL emitted from the SOI surface at room temperature compared to the Czochralski (CZ) silicon, as shown in Fig. 2a (blue curve). Another interesting point to note is that the luminescence is broadband and covers the range from 1000 to 1600 nm. The reason for this broadband luminescence is that there are a large number of defects, which are inhomogeneously emitting at different wavelengths. This inhomogeneously broadened emission from a large number of defects combines to give a net broadband PL from the SOI surface, not very different from the one obtained from inhomogeneously broadened III–V quantum dots created by the Stranski–Krastanov growth mode. We designed and fabricated an L3 PhC cavity in SOI material, with different far-field optimization to enhance vertical in- and out-coupling efficiency [18]. The fundamental mode of the cavity occurs around 1550 nm and the defect emission couples into this nano-cavity. The fabricated PhC nanocavities have typical passive *Q*-factors of the order of 10,000—(linewidth of 0.15 nm), measured by resonant scattering [22]. This coupling of the defect emission to the cavity enhances the luminescence by a factor of up to 300, due to a combination of the Purcell effect and the directional enhancement of the emission via the cavity mode [23]. In this way, we get a bright and narrow (<1 nm) emission line at room temperature from the PhC nanocavity at 1550 nm, which corresponds to the fundamental mode of the cavity as shown in Fig. 2b. In addition to the fundamental mode at 1550 nm, there are six other excited higher order modes. These experimentally measured modes are in perfect agreement with the theoretical calculations, carried out by the Guided Mode Expansion method (GME) [24], as shown in Fig. 2b. We notice that the Q_c extracted from PL measurements is reduced with respect to the one obtained by resonant scattering, i.e. $Q_c=3000$ for the fundamental L3 PhC cavity mode. Such a

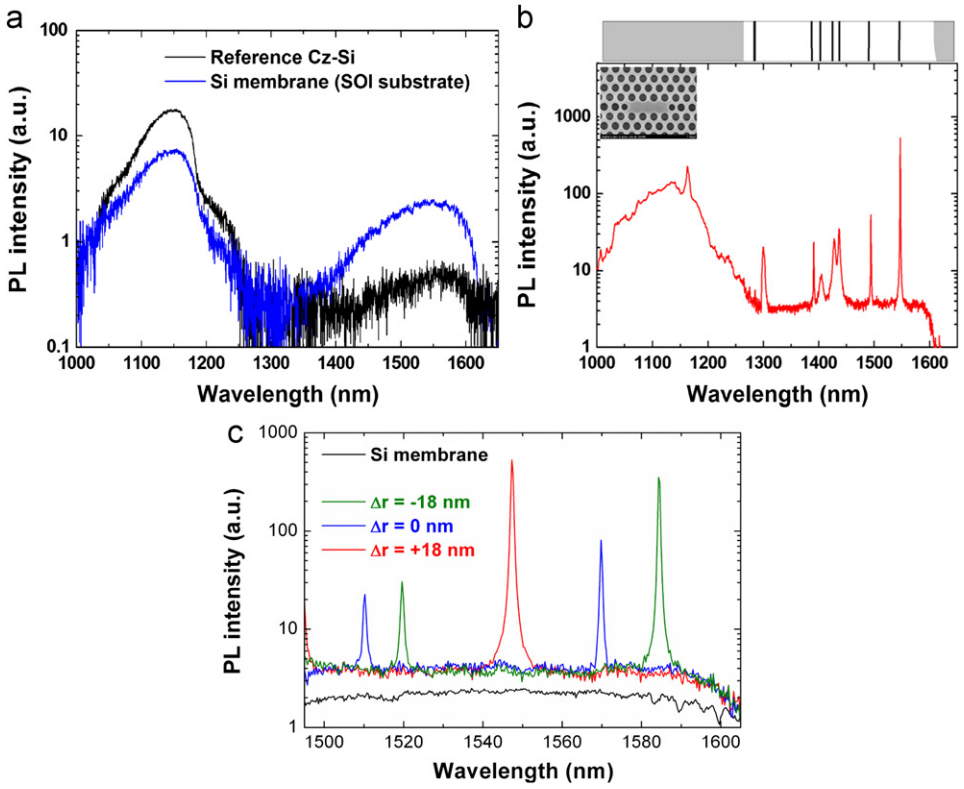

Fig. 2. (a) Comparison of the PL of a Si membrane in a SOI substrate with that of CZ–Si at room temperature, (b) PL spectrum of a PhC L3 nanocavity with $\Delta r = +18$ nm; the top panel shows the wavelengths of the cavity modes, calculated by the GME method; in the inset a SEM image of the cavity is shown. (c) Emission enhancement for 3 different far-field optimization values ($\Delta r = -18$, 0 and $+18$ nm). (For interpretation of the references to colour in this figure legend, the reader is referred to the web version of this article.)

considerable reduction is attributed to the strong free-carrier absorption (FCA) induced by the optical pumping above silicon bandgap. This is also confirmed by the observed blue-shift of the cavity resonances upon increasing the pump power [23]. Nevertheless, the spectral density of the emission from the fundamental mode is comparable to that arising from the silicon band-edge.

From the experimentally measured PL enhancement factor, we can estimate the value of the Purcell factor to be equal to 12 using the following equation:

$$F_p = \frac{\gamma}{\eta_{cavity}/\eta_{membrane}} \tag{3}$$

where γ is the experimentally measured PL enhancement factor, while η_{cavity} and $\eta_{membrane}$ are the light collection efficiencies from the resonance cavity and un-patterned silicon membrane, respectively.

The experimentally measured values of γ for far-field optimization (Δr) of $+18$ nm (red), 0 nm (blue) and -18 nm (green) was 300, 60 and 250, respectively, as shown in Fig. 2c.

The value of $\eta_{membrane}$ is calculated by simple geometrical considerations as shown in Fig. 3, leading us to the following expression:

$$\eta_m = \frac{\Omega}{2\pi} = \int_0^{2\pi}\int_0^{\theta} \sin\theta' \, d\theta' \, d\phi = 1 - \cos\left[\sin^{-1}\left(\frac{NA}{n}\right)\right] = 0.036 \tag{4}$$

here n is the effective refractive index of silicon slab, taken as 3 and $NA = 0.8$ is the numerical aperture of the collection objective.

The values of η_{cavity} for three different far-field optimizations, $\Delta r = -18$ nm, 0 nm and $+18$ nm were calculated to be 0.9, 0.2 and 0.8, respectively, by finite-difference time-domain (FDTD) simulations. Using these values in Eq. (3), we obtain Purcell factor values in the range 10–12 for these three different cases. This consistent value of the Purcell factor for three different far-field optimization values indicates the authenticity of the calculation model.

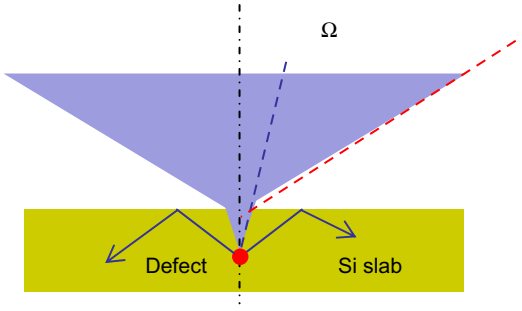

Fig. 3. Schematic of geometrical considerations taken for calculation of collection efficiency.

The observation of such a strong Purcell enhancement gives a clear indication as to the nature of the emission; even though we observe a broad linewidth of emission between 1400 and 1600 nm, it is clear that the emission must be caused by individual, narrow linewidth emitters that are spectrally distributed over the 200 nm bandwidth. In fact, while it is not possible to directly measure the emitters' linewidth by spectroscopic means, we can give a rough estimate of its upper limit using the simplified expression for the Purcell enhancement in Eq. (2). Given a measured $F_p = 12$ and a $Q_c = 3000$ we get $Q_e \geq 160$, implying an emitter linewidth of less than 10 nm at room temperature. A more accurate estimation would require the calculation of the Purcell factor as a convolution, taking into account the spatial distribution of the emitters within the cavity mode profile, which

would possibly further reduce the above upper limit, as will be done in the future analysis.

The Purcell effect has multiple benefits based on the fact that it reduces the radiative lifetime; the shorter lifetime not only enhances the PL but also gives temperature stability to the emission. The temperature stability arising from Purcell enhancement can be understood from the following equation for the radiative efficiency η_{rad}:

$$\eta_{rad} \propto \frac{\tau_{nonrad}}{\tau_{rad}+\tau_{nonrad}} \propto \frac{\tau_{nonrad}}{(\tau_{rad,0}/F_P)+\tau_{nonrad}} \quad (5)$$

where F_p is the Purcell factor, τ_{rad} is the radiative recombination time, $\tau_{rad,0}$ the recombination time in absence of Purcell enhancement and τ_{nonrad} the non-radiative recombination time. The non-radiative recombination time is given by effects such as surface and Auger recombination, all of which are temperature dependent, so when the temperature is increased, τ_{nonrad} typically decreases and the emission is quenched. If the Purcell factor is high, however, the radiative recombination time becomes competitive with the non-radiative time, which leads to a reduced dependence of the radiative efficiency on temperature. This allows us to maintain the on-resonance emission efficiency into higher temperatures, as shown in Fig. 4, which is rather unique amongst the emission enhancement techniques used for silicon; typically, the emission from silicon quenches very quickly with an increase in temperature, as seen for the emission of erbium in silicon [25]. The PL quenching due to the absence of the Purcell effect is also obvious from Fig. 4, where the PL is dramatically quenched in the off-resonance case. Since we measure the Purcell factor of 12, which is relatively high, we do observe a strong stabilization of the emission with temperature. Clearly, this observed stabilization can only occur if the radiative time constants τ_{rad} and τ_{nonrad} are of a similar order of magnitude. Given that the non-radiative lifetime in our photonic crystal structures is known to be of order 50–500 ps [26,27], this suggests that the Purcell-enhanced radiative lifetime of the defect emission is of the same order of magnitude and the native lifetime of the defect emission, $\tau_{rad,0}$, is in the nanosecond regime and hence comparable to III–V quantum dots. This very short lifetime is rather remarkable and so far unreported. We have not yet been able to confirm this lifetime directly, as it requires time-resolved PL measurements with sub-ns resolution, but hope to report on this in the future work.

The observed enhancement of luminescence from silicon via the Purcell effect gives rise to a silicon nano light source, which has all the benefits mentioned in the introduction, i.e. is based on crystalline silicon, has nano size, operates at room temperature, has emission at telecommunication wavelength and can be electrically injected by introduction of pn junctions.

To this end, we recorded the luminescence signal as a function of pump power (Fig. 5). From the graph, it is clear that the laser action is not yet achieved; however, following an initial linear dependence of output power on input power, we observe saturation once the pump power exceeds 1 mW. We observe a blue shift in the resonance wavelength, indicating that the saturation is caused by free carrier absorption (FCA) [23]. The saturation behaviour shows that the FCA is the dominant loss mechanism, and that there is a need to enhance the emission from the nanocavity even further before laser action can be observed. It is also possible that the transition itself is saturating, though we believe the effects of FCA to be dominant.

5. Improvements—increase hydrogen defects in silicon

Since we have now observed enhanced photoluminescence based on the *unintentional* inclusion of hydrogen defects in the Smart Cut™ process, we believe that the *intentional* introduction of defects created by hydrogen would increase the PL even further. Such defects could be introduced either by ion implantation or by an exposure to hydrogen plasma. The creation of defects by hydrogen plasma treatment or ion implantation, and its effect on the PL from silicon, has been investigated previously by a number of different groups [6,28–33]. In Ref. [31], for example, it is shown that the in-diffusion of hydrogen into single crystalline silicon creates platelets, which are stabilized by hydrogen via the formation of H–Si bonds. These platelets are believed to be created by in-diffusion of hydrogen only and are not related to plasma damage. The corresponding midgap electronic levels thus created are considered to be responsible for the luminescence. This claim is contradicted in Refs. [32,33], where no broadband PL was observed from hydrogen in-diffusion only. Instead, the authors state that it is necessary to create defects via plasma damage in order to observe broadband emission. Furthermore, they report that the luminescence arises from the radiative recombination at intrinsic microdefects created by plasma treatment, rather than from hydrogen stabilized platelets formed by the hydrogen in-diffusion as claimed in Ref. [31]. In Ref. [33], two broadband PL bands are observed that are centred at 1.45 μm and 1.3 μm; these bands are associated with bound exciton recombination at donor or acceptor and donor–acceptor pairs within the strain field surrounding the microdefects created by the plasma treatment. In the same work, small dark spot-like features were also observed by TEM; these dark spots exhibit large strain fields

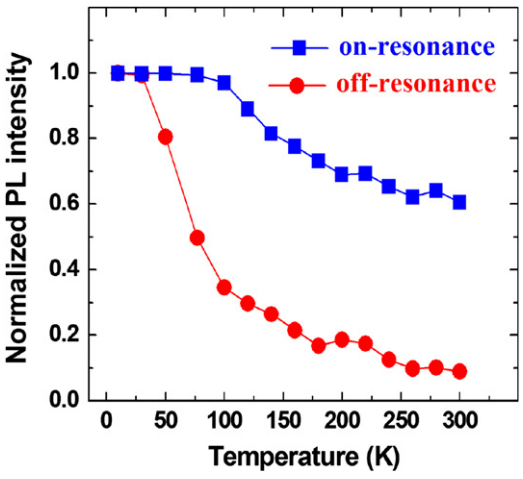

Fig. 4. Temperature stability due to the Purcell effect for on-resonance PL in the cavity with a far-field optimization $\Delta r = +18$ nm.

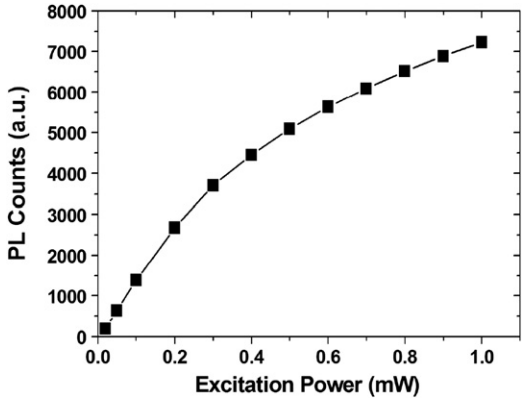

Fig. 5. Pump power dependence of emission from silicon photonic crystal nanocavity.

related to the extended defects. The authors conclude that the PL signal is associated with these small dark spots and the strain associated with these spots is considered to be responsible for the energy shift of the PL band from the band -edge. The exact nature of these defects and the origin of broadband PL are still not confirmed, but the strongest indication is that the broadband emission arises from these defects.

In addition to an investigation of the nature of the defects and the origin of the PL signal from Si, a detailed investigation of the different types of bonds created by the incorporation of hydrogen into silicon (silicon–hydrogen, silicon-vacancy and interstitial silicon–hydrogen) by Raman spectroscopy has also been reported [34]. Although there are clear differences in explanation of the exact nature of the defects, it is now well established that hydrogen plasma treatment or ion implantation causes radiative recombination by a combination of defects and the presence of hydrogen [32]. Therefore, by implementing a suitable hydrogen plasma treatment or ion implantation to increase the amount of optically active hydrogen related defects, we expect to increase the PL from our silicon photonic crystal nanocavity even further.

6. Conclusions

In conclusion, we have demonstrated a narrow emission line from crystalline silicon at room temperature by coupling the defect emission from silicon with a PhC nanocavity and utilizing the Purcell effect. This emission line is in the 1.4–1.6 μm wavelength window and its intensity is comparable to that at the silicon band-edge. No sign of optical gain or stimulated emission is observed, however, which we attribute to the presence of a strong free carrier absorption. A number of conclusions can be drawn regarding the nature of these emitters: (a) they are of bandwidth comparable to that of photonic crystal cavity and inhomogeneously broadened, as the Purcell enhancement would not be observable otherwise; (b) they have a very short radiative lifetime, probably in the nanosecond regime, as determined from the weak temperature dependence and the known non-radiative lifetime (≈ 100 ps); (c) the absence of lasing and observed saturation with pump power suggests that there are too few defects to provide an overall net gain.

To overcome free carrier absorption and achieve gain, we have discussed the possibility of introducing additional defects by either hydrogen implantation or by hydrogen plasma treatment. The demonstrated nano-emitter is small, has very narrow linewidth emission, operates at room temperatures and can be pumped electrically by incorporation of pn junctions around the cavity. This approach is a major step forward towards realising an electrically pumped, silicon nanolaser that operates at room temperature.

Acknowledgements

We are grateful to F. Priolo and P. Cardile from *CNR-IMM MATIS and Dipartimento di Fisica e Astronomia, Università di Catania, Italy*, for useful discussions. This work was supported by Era-NET NanoSci LECSIN project coordinated by F. Priolo, by the Italian Ministry of University and Research, FIRB Contract no. RBAP06L4S5 and the UK EPSRC UK Silicon Photonics project. The fabrication was carried out in the framework of NanoPiX (see http://www.nanophotonics.eu).

References

[1] S.G. Cloutier, P.A. Kossyrev, J. Xu, Nat. Mater. 4 (2005) 887.
[2] W.L. Ng, M.A. Lourenco, R.M. Gwilliam, S. Ledain, G. Shao, K.P. Homewood, Nature 410 (2001) 192.
[3] H.S. Rong, M. Paniccia, et al., Nature 433 (2005) 292.
[4] H. Ennen, G. Pomrenke, A. Axmann, K. Eisele, W. Haydl, J. Schneider, Appl. Phys. Lett. 46 (1985) 381.
[5] F. Priolo, G. Franzò, S. Coffa, A. Carnera, Phys. Rev. B 57 (1998) 4443.
[6] G. Davies, Phys. Rep. 176 (1989) 83.
[7] J. Bao, M. Tabbal, T. Kim, S. Charnvanichborikarn, J. Williams, M.J. Aziz, F. Capasso, Opt. Express 15 (2007) 6728.
[8] E.Ä.O. Sveinbj Ärnsson, J. Weber, Appl. Phys. Lett. 69 (1996) 2686.
[9] M. Fujita, B. Gelloz, N. Koshida, S. Noda, Appl. Phys. Lett. 97 (2010) 121111.
[10] N. Hauke, T. Zabel, K. Mueller, M. Kaniber, A. Laucht, D. Bougeard, G. Abstreiter, J.J. Finley, Y. Arakawa, New J. Phys. 12 (2010) 053005.
[11] S. Iwamoto, Y. Arakawa, Appl. Phys. Lett. 91 (2007) 211104.
[12] E.M. Purcell, Phys. Rev. 69 (1946) 681.
[13] J.-M. Lourtioz, H. Benisty, V. Berger, Photonic Crystals: Towards Nanoscale Photonic Devices, Springer–Verlag, ISBN 3540783466, 2008–06.
[14] J.-M. Gérard, Top. Appl. Phys. 90 (2003) 269.
[15] T. Akahane, T. Asano, B.-S. Song, S. Noda, Nature 425 (2003) 944.
[16] L.C. Andreani, D. Gerace, M. Agio, Photonics Nanostruct. Fund. Appl. 2 (2004) 103.
[17] N.-V.-Q. Tran, S. Combrié, A. De Rossi, Phys. Rev. B 79 (2009) 041101.
[18] S.L. Portalupi, M. Galli, C. Reardon, T.F. Krauss, L. O'Faolain, L.C. Andreani, D. Gerace, Opt. Express 18 (2010) 16064.
[19] D. Recht, F. Capasso, Michael J. Aziz, Appl. Phys. Lett. 94 (2009) 251113.
[20] E. Simoen, C. Claeys, E. Gaubas, H. Ohyama, Nucl. Instrum. Methods—Phys. Res. Sect. A 439 (2000) 310.
[21] P.J. Dean, J.R. Haynes, W.F. Flood, Phys. Rev. 161 (1967) 711.
[22] M. Galli, S.L. Portalupi, M. Belotti, L.C. Andreani, L. O'Faolain, T.F. Krauss, Appl. Phys. Lett. 94 (7) (2009) 071101.
[23] R. Lo Savio, S.L. Portalupi, D. Gerace, A. Shakoor, T.F. Krauss, L. O'Faolain, L.C. Andreani, M. Galli, Appl. Phys. Lett. 98 (2011) 201106.
[24] L.C. Andreani, D. Gerace, Phys. Rev. B 73 (2006) 235114.
[25] S. Coffa, G. Franzò, F. Priolo, A. Polman, R. Serna, Phys. Rev. B 49 (1994) 16313.
[26] T. Tanabe, M. Notomi, S. Mitsugi, A. Shinya, E. Kuramochi, Appl. Phys. Lett. 87 (2005) 151112.
[27] P. Barclay, K. Srinivasan, O. Painter, Opt. Express 13 (2005) 801.
[28] J.M. Hwang, et al., J. Appl. Phys. 57 (1985) 5275.
[29] L.T. Canham, M.R. Dyball, W.Y. Leong, M.R. Houlton, A.G. Cullis, P.W. Smith, Mater. Sci. Eng. B 4 (1989) 41–45.
[30] A Henry, B Monemar, J.L Lindstrom, T.D Bestwick, G.S Oehrlein, J. Appl. Phys. 70 (10) (1991).
[31] N.M. Johnson, F.A. Ponce, R.A. Street, R.J. Nemanich, Phys. Rev. B 35 (1987) 4166.
[32] J. Weber, Physica B 170 (1991) 201–217.
[33] M. Singh, J. Weber, M. Konuma, Physica B 170 (1991) 218–222.
[34] W. Dungen, R. Job, Y. Ma, Y.L. Huang, T. Mueller, W.R. Fahrner, L.O. Keller, J.T. Horstmann, H. Fiedler, J. Appl. Phys. 100 (2006) 034911.